Ensuring Soft Switching During Transient Operations of Wireless Power Transfer Systems with Frequency Control

[*]Shuxin Chen, [†]Jiayu Zhou, [*]Yaohua Li, [#]Giuseppe Guidi, [†,#]Jon Are Suul, and [*]Yi Tang
[*]School of Electrical and Electronic Engineering, Nanyang Technological University, Singapore
[†]Department of Engineering Cybernetics, Norwegian University of Science and Technology, Trondheim, Norway
[#]SINTEF Energy Research, Trondheim, Norway
yitang@ntu.edu.sg

***Abstract*—The high switching frequency of wireless power transfer systems makes soft switching important due to switching losses. In the current literature, numerous solutions have been proposed for maintaining soft switching within the entire operating range. However, this study shows that variable frequency control can cause loss of zero voltage switching (ZVS) during system transients, even if soft switching during steady-state operation is ensured. The causes of this phenomena are analyzed thoroughly and two approaches to address such issue are discussed. Firstly, a limitation on the changing rate of the frequency can alleviate the issue. Secondly, phase advance control could also be possible, although this approach requires further studies. Results from both simulations and laboratory experiments are presented to verify the analysis and the control method proposed to avoid losing ZVS during transient conditions.**

Keywords—Wireless power transfer, zero voltage switching, soft switching, frequency control

I. INTRODUCTION

Wireless power transfer (WPT) technologies have been widely studied in recent years for the inherent advantages over traditional wired systems, such as safety in terms of reduced risk of electric shock and reduced maintenance requirements by avoiding mechanical wear and tear [1, 2]. Among all WPT techniques, inductive power transfer (IPT) is one of the most promising solutions. In principle, IPT systems utilize a pair of coils to achieve contactless power transmission through magnetic fields.

To obtain a sufficiently long transmission range with moderate coil size, the operating frequency in an IPT system is normally high, e.g., 80-90 kHz for vehicle charging according to the SAE standard [3] and hundreds of kHz for mobile device charging according to the Qi standard [2]. However, the high operating frequency introduces several concerns, such as system losses and noise. With soft switching, both switching losses and noise can be greatly reduced. Hence, one critical design consideration is to maintain soft switching over the entire operating range, i.e., the designed output power range and transmission distance. In general, achieving full-range soft switching is important to reduce system size and loss.

This work was part of the research program of Maritime Research Between Singapore (Singapore Maritime Institute) and Norway (Research Council of Norway), which was supported by the Singapore Maritime Institute under Project SMI-2019-MA-02 and Research Council of Norway under Project number 294871.

Using a dc-dc converter is a common solution for regulating the power flow in response to variations in the load and the magnetic coupling [4, 5]. Full-range soft switching for the high frequency resonant converters can be achieved by the design of the IPT compensation network and operating frequency. However, the need of a dc-dc converter is a drawback as system costs and size could be increased. Although it is possible to directly control the inverter and rectifier to achieve output power control without a dc-dc converter, a more careful design is required to avoid the loss of soft switching due to the control. For example, the joint control of inverter and rectifier phase shift angle presented in [6] achieves full-range soft switching. In [7], pulse density modulation (PDM) is used to regulate the system power. With the use of a zero voltage switching (ZVS) branch, soft switching can be ensured regardless of the variations of the coupling coefficient and load. In [8], a novel variable frequency control is presented. By properly designing the subresonant range of the system, the inverter can regulate output power against a wide range of coupling coefficient variation while remaining ZVS. Moreover, the adaptive frequency control in [8] can maintain zero input phase angle and output power control. Generally, there are numerous works addressing the full range ZVS issue in the literature.

Most of the existing works can ensure soft switching in steady state, which is the most critical. Nonetheless, it is possible for the system to experience hard switching during transient conditions, such as a rapid change of load or coupling coefficient. In principle, losing soft switching during transients will not lead to a large power loss that causes thermal problems as the duration is essentially short. However, voltage spikes caused by the hard switching is harmful. Hard switching noise can also affect gate driver circuit, where, in the worst case, switching devices can be accidentally turned on that could cause short-circuit. EMI problems to surrounding devices is also a concern. Therefore, losing soft switching during system transients is unwanted. However, this issue is barely studied in the literature.

In this study, it is found that frequency control can experience phase drops during system transients. The phase drops may cause hard switching, even though soft switching can be achieved in steady state. To illustrate the problem, the subresonant frequency design in [8] will be used as an example. The reason and condition of such phenomenon is thoroughly analyzed in this article. Also, it has been shown that limiting frequency change rate can alleviate the problem. Performing

phase advance may also be beneficial, but more studies are required as an aggressive phase advance design can cause instability. Experimental results have been provided for verification.

II. System Analysis

A. Typical System Structure

A series-series (S-S) compensated IPT system will be used to study the system behavior, where the circuit diagram is given in Fig. 1. The dc input voltage, V_{in}, is converted to ac voltage through the inverter, i.e., Q_1-Q_4, at the operating frequency f_o. The rectifier, i.e., D_1-D_4, is connected to the constant-voltage load, of which the voltage is V_o and the equivalent load resistance is R_L. L_p, L_s, and M_{ps} represent the primary side self-inductance, secondary side self-inductance, and the mutual inductance, correspondingly. C_p and C_s are the compensation capacitors for the primary side and secondary side. Similarly, R_p and R_s refer to the equivalent series resistance of the primary side and secondary side circuit. Accordingly, ω_p and ω_s are the primary and secondary side resonant frequencies respectively, as defined by

$$\omega_p = \frac{1}{\sqrt{L_p C_p}}, \tag{1}$$

$$\omega_s = \frac{1}{\sqrt{L_s C_s}}. \tag{2}$$

In actual designs, there would be $\omega_s > \omega_p$ which is beneficial to realize inverter ZVS operations [4].

B. ZVS Operation for Inverter

For soft switching of Si MOSFET, SiC MOSFET, and GaN FET, ZVS turn on is crucial, to avoid excessive switching losses. In theory, ZVS turn on requires V_{ds}, the voltage across one switching device, to be nearly zero before turning on, which can be realized by having a negative current to discharge device equivalent output capacitance C_{oss}. The required current is related to the device model and deadtime, where detailed analyses can be found in [9].

For simplification without the loss of generality, the inverter is considered to achieve ZVS as long as the inverter current i_{Lp} is lagging inverter voltage u_{in}. Therefore, if the equivalent impedance Z_{send} seen by the inverter is inductive, i.e., $\mathrm{Arg}(Z_{send})>0$, the inverter is considered achieving ZVS, representing soft switching. For example, the subresonant frequency design in [8] uses a detune factor to adjust ω_p and ω_s to maintain $\mathrm{Arg}(Z_{send})>0$ under all possible operating conditions to ensure full range ZVS. The system characteristics provided in Fig. 2 shows that subresonant frequency control can maintain power regulation and ZVS against a wide coupling coefficient range.

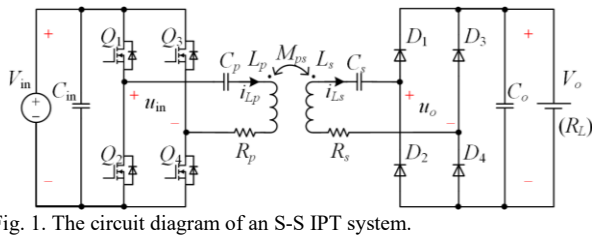

Fig. 1. The circuit diagram of an S-S IPT system.

C. Losing ZVS During Frequency Change

Even with the characteristics in Fig. 2, it is found that ZVS can be lost during system transients. The issue is illustrated and explained from indicated waveforms in Fig. 3. After a step change is applied to the system frequency, the inverter voltage V_p changes immediately, while the inverter current I_p gently changes to the new frequency, as the current is influenced by a relatively large time constant due to the resonators. Hence, during the dynamic process, there is naturally a frequency difference between V_p and I_p, leading to a phase difference and the loss of ZVS.

Typically, the loss of ZVS tends to occur when f_o increases. At the first cycle of the frequency step change, it can be assumed that I_p remains unchanged, and the phase change $\Delta\varphi$ can be derived as:

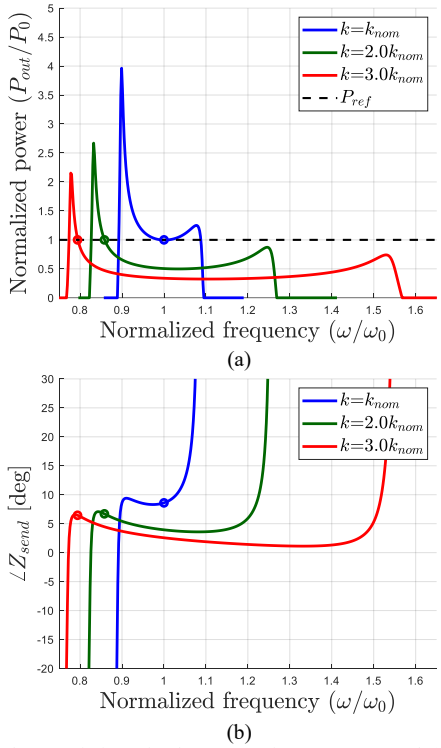

Fig. 2. Characteristics of subresonant frequency control (a) power (b) input phase angle.

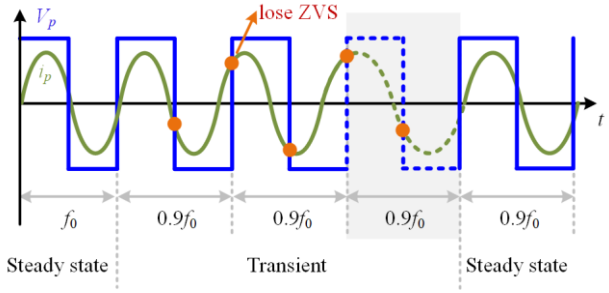

Fig. 3. The indication diagram of system waveforms with a frequency step change.

$$\frac{\Delta f}{f_0} = \frac{\Delta \varphi}{2\pi} \tag{3}$$

Accordingly, for the $-0.1\Delta f$ in Fig. 3, the first cycle phase change is 36°. In the following cycles, I_p will follow the new operating frequency and the each cycle phase change will be smaller than 36°. If the accumulated phase difference is larger than the initial phase, the loss of ZVS can be observed. Although only three cycles are drawn in Fig. 3 to describe the dynamic process, the cycle in dashed line represents multiple cycles as actual dynamic process can last for a certain duration, which is determined by system dynamic response. As an extreme example, one can assume that I_p remains unchanged for a long term due to the slow response, the phase change at the n^{th} cycle will be $n\times36°$ with the $-0.1\Delta f$.

Clearly, the indicated phase change can result in the loss of ZVS. Generally, according to (3), the loss of ZVS could occur at the first cycle whenever the system operating frequency experiences a step change, regardless of system operating points. Depending on the system dynamic response, the loss of ZVS can occur and last for a certain duration.

In principle, the loss of ZVS during system transients will not cause thermal issue as the dynamic process is relatively short. However, a large switching spike can happen due to hard switching. The hard switching noise can also threaten gate driver circuit and nearby electronic devices. Hence, it is beneficial if the loss of ZVS during system transients can be avoided.

III. System Modeling and Analysis

A. Nonlinear Model

In order to further analyze the discussed phenomenon, a time-invariant state-space model is established in this section. Assuming a synchronous reference frame *dq* representation of the state variables with first harmonic approximation, the model can be derived and expressed in the general state-space form as [10]:

$$\dot{\mathbf{x}} = f(\mathbf{x}, \mathbf{u}) \tag{4}$$

with $\begin{cases} \mathbf{x} = [i_{p\text{-}d} \quad i_{p\text{-}q} \quad i_{s\text{-}d} \quad i_{s\text{-}q} \quad u_{Cp\text{-}d} \quad u_{Cp\text{-}q} \quad u_{Cs\text{-}d} \quad u_{Cs\text{-}q}]^T \\ \mathbf{u} = [u_{p\text{-}d} \quad u_{p\text{-}q} \quad \omega_o \quad V_{out}]^T \end{cases}$.

The differential equations can be found in the appendix.

To intuitively reflect the relationship between the input impedance angle and the input states, the output of the model in this paper is set as:

$$\mathbf{y} = g(\mathbf{x}, \mathbf{u}) \tag{5}$$

with $\mathbf{y}=[\varphi]$ which refers to the phase angle φ between the sending voltage and the sending current, i.e., $\text{Arg}(Z_{\text{send}})$.

Defining the phase angle of the input sending voltage as 0, the *dq*-frame representation of the input voltage can be obtained as:

$$\begin{cases} u_{p\text{-}d} = \dfrac{2\sqrt{2}}{\pi} V_{\text{in}} \\ u_{p\text{-}q} = 0 \end{cases} \tag{6}$$

In this case, the phase of the sending current is also the input impedance angle, expressed as:

$$\varphi = \arcsin\left(\frac{i_{p\text{-}q}}{\sqrt{i_{p\text{-}d}^2 + i_{p\text{-}q}^2}} \right) \tag{7}$$

Therefore, with the developed model, the dynamic response of φ can be studied.

B. Analysis and Discussion

Based on the nonlinear model, a step change in operating frequency is applied to the system to study the system dynamic response. Results have been collected in Fig. 4, where case 1, 2, and 3 refers to a frequency step from f_o to 0.97 f_o, from 0.97 f_o to 0.94 f_o, and from 0.94 f_o to 0.91 f_o, respectively. It can be found that there is an undershoot phenomenon in $i_{p\text{-}q}$, which causes the input impedance of the system to become capacitive in a short time. Therefore, the system may lose ZVS in the process of frequency change. As the operating frequency moves away from the resonant frequency, the system loses ZVS more severely and for longer. According to Fig. 4, the input phase drops to as low as −20° in the case 1, where the steady state angle is about 6°. Clearly, severe hard switching can be observed during the transient process.

Meanwhile, according to the case 3 in Fig. 4, even with the transient phase drop, φ merely becomes negative, as the steady state value of φ is close to the phase drop. Hence, one straight forward solution to avoid hard switching is to increase initial φ such that φ is higher than the worst-case phase drop, e.g., initial φ>30°. From [8], modifying the detuning factor is a valid way

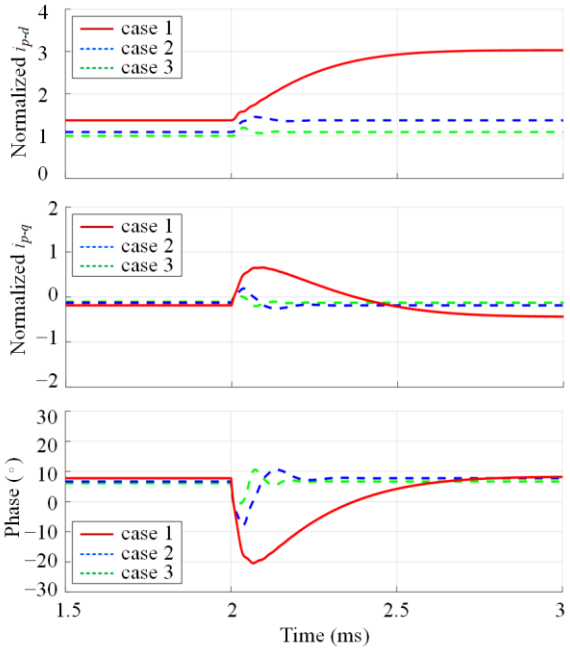

Fig. 4. Results from the mathmatical model.

to increase φ. However, the solution is not cost-effective as a high nominal φ also indicates higher reactive power, indicating that steady state performance is sacrificed. In actual design, initial φ is usually kept small, which means that the capability to withstand phase drops without hard switching is limited.

IV. Proposed Solutions

A. Limiting Frequency Change Rate

In normal systems with variable frequency control, the system operating frequency is determined by PI (proportional-integral) controller, and a step change can occur if there is an error on the controlled output, e.g., system power. According to (3), the value of $\Delta\varphi$ is related to Δf, indicating that suppressing Δf is beneficial to the reduction of $\Delta\varphi$. Hence, limiting the changing rate of frequency, e.g., turning the step change into a ramp, can help avoid the loss of ZVS.

Fig. 5 demonstrates the results from the mathematical model and simulation with different frequency disturbances. Clearly, limiting the frequency change rate is a valid solution. From Fig. 5 (c), the phase angle can be maintained positive during the entire dynamic process.

B. Phase Advancing

Another possible solution is to temporarily raise the input side phase angle, which is called phase advancing in this article. Fig. 6 (a) shows the regular system waveforms under frequency step change. In Fig. 6 (b), the second cycle is shifted to the left, which is realized by shortening the first cycle. As a result, φ is temporarily increased, which compensates the effect of the phase drop caused by frequency changes. Similarly, Fig. 6 (c) shows another way to realize phase advancing. Both ways can increase φ and can be selected based on the way of pulse width modulation (PWM) signal generation.

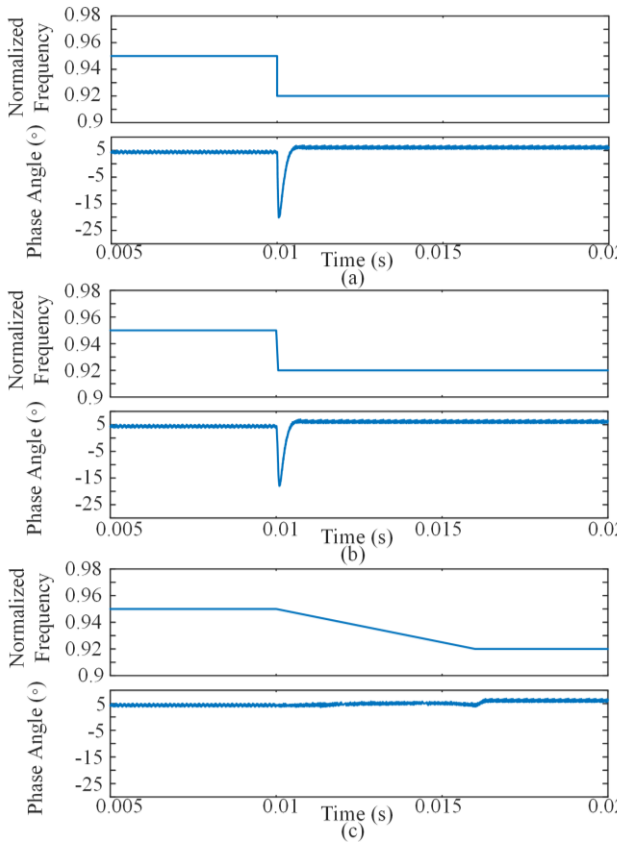

Fig. 5. Simulation results with a (a) step change (b) fast ramp change (c) slow ramp change.

From (3), if the phase advancing angle, written as θ_{PA}, satisfies

$$\varphi_o + \theta_{PA} > 2\pi \frac{\Delta f}{f_o}, \tag{8}$$

with φ_o being the initial phase angle, loss of ZVS at the first cycle can be prevented. In actual designs, φ_o is designed to be positive (Z_{send} being inductive) through detuning, where the minimum φ_o needed would be subject to the switching current required for ZVS. The detailed design of φ_o and detuning parameters can be found in [8].

Phase advancing can be activated multiple times to prevent the loss of ZVS. It is also possible to use phase advancing together with the change rate limiting solution to achieve better results. However, system instability can occur if phase advancing is extremely aggressive, i.e., θ_{PA} is excessive. Hence, the impact of both solutions to the system requires a further study. For verification, experimental results are provided in the following section.

V. Experimental Verification

A. Experiment Setup

An experimental platform following the structure in Fig. 1 is developed, where a photo and parameters are given in Fig. 7 and Table I. The coil diameter is 300*300 mm, and the air gap is around 125 mm. In the experiment, a constant voltage load is

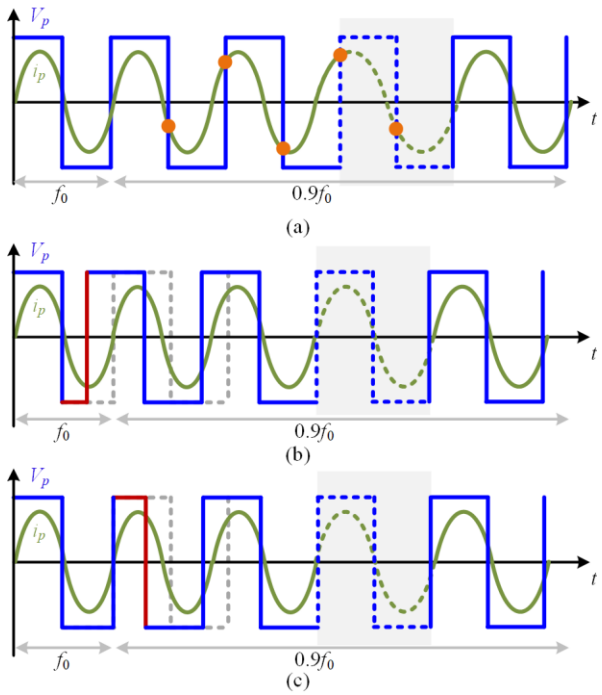

Fig. 6. Indication waveforms with a frequency step change (a) original (b) phase advancing mode A (c) phase advancing mode B.

used to simulate a battery load. To realize wide range ZVS operations, detuning is applied to the resonator, and input voltage is slightly higher than output voltage [8].

B. Experimental Results

In principle, the ZVS status of one semiconductor device should be inspected by comparing the corresponding gate driver signal V_{gs} and the drain-source voltage V_{ds}. However, due to the long time span it is difficult to show V_{gs} and V_{ds} clearly in the figure during the dynamic conditions for illustrating the ZVS status. Instead, the phase information calculated from experimental data with MATLAB will be provided, which should be easier to view. The phase is obtained by capturing the time difference between the zero crossing points of the inverter voltage and current. Although the accuracy of the calculated phase angle can be affected by the ringing on ac currents, the overall tendency for the change of phase signal can be well reflected.

The steady state waveforms at different frequencies are provided in Fig. 8. It can be seen that the input phase angle is always positive in steady state, which is beneficial for ZVS operations. Afterward, a step frequency change, from 80 kHz to 77.5 kHz, is applied to the system. In Fig. 9, input phase angle experiences a down-swing and becomes negative, and the lowest phase angle is about −18°. Hard switching can be observed due to the negative phase angle. As a comparison, a ramp rate is applied to the controller such that frequency will change from 80 kHz to 77.5 kHz gradually within about 5 ms. The results in Fig. 10 indicate that input phase angle is kept positive with the frequency change.

In the experiment, the loss of ZVS issue is not as severe as in Fig. 5, which can be because of the different system

Table I. System Parameters

Symbol	Description	Value
L_p	primary-side coil inductances	~130 μH
L_s	secondary-side coil inductances	~125 μH
M_{ps}	mutual inductance	~40 μH
C_p	primary-side series capacitance	~28 nF
C_s	secondary-side series capacitance	~28 nF
V_{in}	Input voltage	26V
V_o	Output voltage	25V

Fig. 7. A photo of IPT coils used in the experiment.

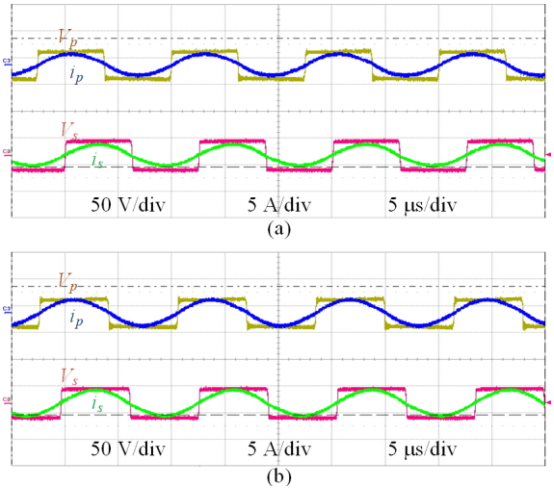

Fig. 8. Experimental waveforms at the steady state (a) 80 kHz (b) 77.5 kHz.

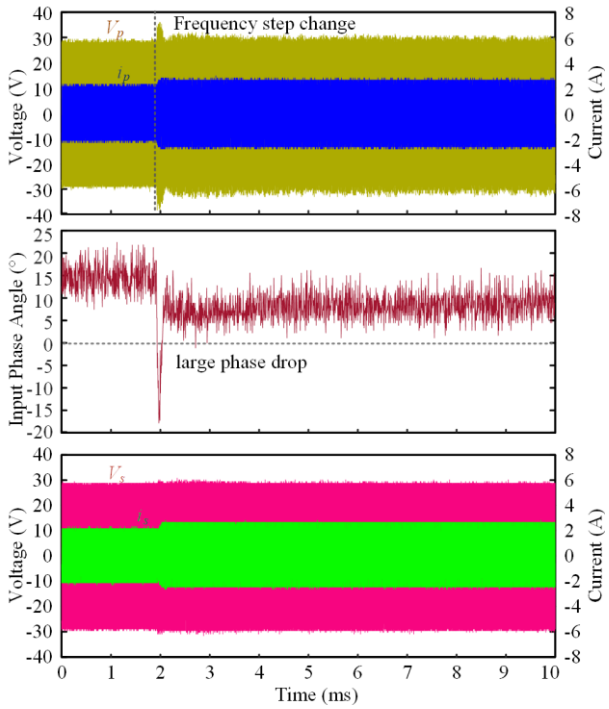

Fig. 9. Experimental waveforms of system dynamic with a frequency step change.

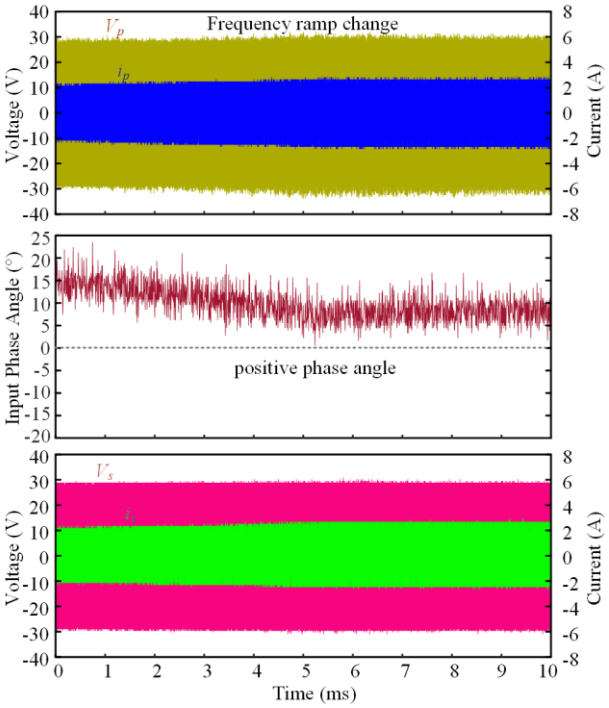

Fig. 10. Experimental waveforms of system dynamic with a frequency ramp change.

parameters and operating points. For instance, the output power difference between the two indicated frequency is much smaller than the one in Fig. 5. In general, limiting the frequency change rate is a valid solution to avoid the loss of ZVS during system dynamic processes.

The phase advancing approach is also evaluated in experiment. In Fig. 11, phase advancing is triggered once at the second cycle, and the input phase angle is successfully increased temporarily. The advanced time is about 800 ns, which is deliberately set to be large such that the phase change can be clearly observed. The actual performance of phase advancing against the loss of ZVS issue will be studied in the future.

VI. Conclusions and Future Works

In this article, the problem of losing ZVS during system transients for IPT systems is studied. It has been shown that, for variable frequency control, the system can experience phase drops during the dynamic process. As a result, ZVS can be lost during the process, even in the situation that ZVS can be maintained under steady state. The reason is explained, and a mathematical model is established to describe the issue. To address the problem, limiting the frequency change rate is a valid solution. Temporarily increasing input phase angle through phase advancing can also be a potential solution. Experimental results have been provided for verification. In general, the loss of ZVS problem can happen for variable frequency control when system frequency changes quickly. The severity and potential solutions to the problem for different frequency control strategies will be studied by more comprehensive analyses in future works.

Appendix

The below differential equations have been used in the mathematic model:

$$\frac{di_{p-d}}{dt}=\omega_o i_{p-q}-\frac{R_p}{L_{\alpha p}}i_{p-d}-\frac{M_{ps}R_s}{L_{\alpha p}L_s}i_{s-d}-\frac{1}{L_{\alpha p}}v_{Cp-d}$$
$$-\frac{M_{ps}}{L_{\alpha p}L_s}v_{Cs-d}+\frac{1}{L_{\alpha p}}v_{p-d}-\frac{M_{ps}}{L_{\alpha p}L_s}v_{s-d}$$

$$\frac{di_{p-q}}{dt}=-\omega_o i_{p-d}-\frac{R_p}{L_{\alpha p}}i_{p-q}-\frac{M_{ps}R_s}{L_{\alpha p}L_s}i_{s-q}-\frac{1}{L_{\alpha p}}v_{Cp-q}$$
$$-\frac{M_{ps}}{L_{\alpha p}L_s}v_{Cs-q}+\frac{1}{L_{\alpha p}}v_{p-q}-\frac{M_{ps}}{L_{\alpha p}L_s}v_{s-q}$$

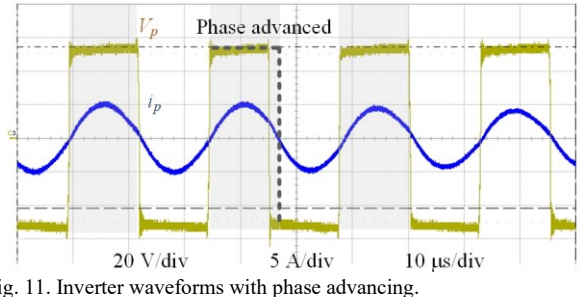

Fig. 11. Inverter waveforms with phase advancing.

$$\frac{di_{s-d}}{dt}=-\omega_o i_{s-q}-\frac{M_{ps}R_s}{L_{\alpha s}L_p}i_{p-d}-\frac{R_s}{L_{\alpha s}}i_{s-d}-\frac{M_{ps}}{L_{\alpha s}L_p}v_{Cp-d}$$
$$-\frac{1}{L_{\alpha s}}v_{Cs-d}+\frac{M_{ps}}{L_{\alpha s}L_s}v_{p-d}-\frac{1}{L_{\alpha s}}v_{s-d}$$

$$\frac{di_{s-q}}{dt}=-\omega_o i_{s-d}-\frac{M_{ps}R_p}{L_{\alpha s}L_p}i_{p-q}-\frac{R_s}{L_{\alpha s}}i_{s-q}-\frac{M_{ps}}{L_{\alpha s}L_p}v_{Cp-q}$$
$$-\frac{1}{L_{\alpha s}}v_{Cs-q}+\frac{M_{ps}}{L_{\alpha s}L_p}v_{p-q}-\frac{1}{L_{\alpha s}}v_{s-q}$$

$$\frac{dv_{cp-d}}{dt}=\omega_o v_{cp-q}-\frac{1}{C_p}i_{p-d}$$

$$\frac{dv_{cp-q}}{dt}=-\omega_o v_{cp-d}+\frac{1}{C_p}i_{p-q}$$

$$\frac{dv_{cs-d}}{dt}=\omega_o v_{cs-q}+\frac{1}{C_s}i_{s-d}$$

$$\frac{dv_{cs-q}}{dt}=-\omega v_{cs-d}+\frac{1}{C_s}i_{s-q}$$

where $L_{\alpha p}=L_p-M_{ps}^2/L_s$, $L_{\alpha s}=L_s-M_{ps}^2/L_p$.

References

[1] Z. Zhang, H. Pang, A. Georgiadis, and C. Cecati, "Wireless Power Transfer—An Overview," in *IEEE Transactions on Industrial Electronics,* vol. 66, no. 2, pp. 1044-1058, Feb. 2019.

[2] S. Y. R. Hui, "Past, present and future trends of non-radiative wireless power transfer," in *CPSS Transactions on Power Electronics and Applications,* vol. 1, no. 1, pp. 83-91, Dec. 2016.

[3] D. Patil, M. K. McDonough, J. M. Miller, B. Fahimi, and P. T. Balsara, "Wireless Power Transfer for Vehicular Applications: Overview and Challenges," in *IEEE Transactions on Transportation Electrification,* vol. 4, no. 1, pp. 3-37, March 2018.

[4] W. X. Zhong and S. Y. R. Hui, "Maximum Energy Efficiency Tracking for Wireless Power Transfer Systems," in *IEEE Transactions on Power Electronics,* vol. 30, no. 7, pp. 4025-4034, July 2015.

[5] H. Li, J. Li, K. Wang, W. Chen, and X. Yang, "A Maximum Efficiency Point Tracking Control Scheme for Wireless Power Transfer Systems Using Magnetic Resonant Coupling," in *IEEE Transactions on Power Electronics,* vol. 30, no. 7, pp. 3998-4008, July 2015.

[6] Y. Jiang, L. Wang, J. Fang, C. Zhao, K. Wang, and Y. Wang, "A Joint Control With Variable ZVS Angles for Dynamic Efficiency Optimization in Wireless Power Transfer System," in *IEEE Transactions on Power Electronics,* vol. 35, no. 10, pp. 11064-11081, Oct. 2020.

[7] H. C. Li, K. P. Wang, J. Y. Fang, and Y. Tang, "Pulse Density Modulated ZVS Full-Bridge Converters for Wireless Power Transfer Systems," in *IEEE Transactions on Power Electronics,* vol. 34, no. 1, pp. 369-377, Jan. 2019.

[8] G. Guidi and J. A. Suul, "Minimizing Converter Requirements of Inductive Power Transfer Systems With Constant Voltage Load and Variable Coupling Conditions," in *IEEE Transactions on Industrial Electronics,* vol. 63, no. 11, pp. 6835-6844, Nov. 2016.

[9] M. A. d. Rooij, "The ZVS voltage-mode class-D amplifier, an eGaN FET-enabled topology for highly resonant wireless energy transfer," in *2015 IEEE Applied Power Electronics Conference and Exposition (APEC)*, 15-19 March 2015, pp. 1608-1613.

[10] E. Torsgård, G. Guidi, and J. A. Suul, "Small-Signal State-Space Analysis of Inductive Battery Charging System in Off-Resonant Operation," *2019 20th Workshop on Control and Modeling for Power Electronics (COMPEL)*, 2019, pp. 1-8, doi: 10.1109/COMPEL.2019.8769678